Dynamic behavior of a valve train system in presence of camshaft errors

TOUNSI M., CHAARI F., WALHA L., FAKHFAKH T., HADDAR M.
Dynamics of Mechanical Systems Research Unit
National School of Engineers of Sfax
TUNISIA
Fakher.chaari@gmail.com

Abstract: - In this paper a dynamic model of cam-follower-rocker-valve system is presented. The lumped parameters model is with 8 degrees of freedom. Camshaft eccentricity and cam profile errors are also modeled and can be introduced in the model to observe their influence. The numerical simulation shows a fluctuation on the acceleration of the valve induced by the motion law exerted by the cam follower mechanism. The presence of eccentricity on camshaft showed a slight influence on the dynamic behavior whereas the cam profile error showed a substantial increase in the vibration levels.

Key-Words: - cam follower , valve train , dynamic behavior, eccentricity, profile error

1 Introduction

Valves in distribution systems of internal combustion engines must ensure a suitable filling of cylinders in gasoline-air mixture for gasoline engines and in air for Diesel engines. On the other hand, for high engine speeds, valves may not have time to return to initial positions. It follows a loss power and in certain cases interference between the valve head and piston causing a broken engine[1,2]. The dynamic behavior of the system camshaft, follower, push-rod and valve is in a great importance in the good working of the system [3]. From design phases, engineers can predict this dynamic behavior as function of the different parameters of the engine valve train components. Several authors were interested in this research field.

Through computer modeling, experimental validation, and robust optimal design strategies David [4] showed that it is possible to develop optimal design to produce optimal valve train systems.

Choi [5] was interested in the elaboration of camshaft lobes profiles using implicit filtering algorithm helping parameter identification and optimization in automotive valve train design

Cardona [6] presented a methodology to design cams for motor engine valve trains using a constrained optimization algorithm in order to maximize the time integral of the valve area opened to gas flow. He observed that profile errors can have a large influence on the dynamic performance of such high-speed follower cam systems

Kim [7] used a lumped mass-spring-damper to predict the dynamic behavior of cam-valve system which gives concordant results compared with experimental tests for the evaluation of contact forces in the system.

Jeon [8] stated that with experimental and simulation results that optimizing a cam profile can increase the valve lift area while reducing the cam acceleration and the peak pushrod force. It can also avoid the jump phenomenon of the follower observed at certain

Teodorescu [9] presented an analysis of a line of valve trains in a four-cylinder, four-stroke in-line diesel engine in order to predict the vibration signature taking into account frictional and contact forces.

Carlini [10] conducted a series of experimental measurements of valve motion of a motorbike engine and identified the effect of backlash in cam kinematic pairs and the ensuing jump phenomenon.

De Wilde [11] was interested in wear affecting valves. He concluded that it is then necessary to reduce the coefficient of friction by adopting the proper material combination.

In this paper, a lumped parameter model of a cam-valve mechanism is developed taking into account Hertzian stiffness between cam and push-rod. The simulation of the dynamic behavior of this mechanism is achieved with and without eccentricity and profile errors on camshaft.

2 Dynamic model of the system

The steering of valves motion relatively to the piston is achieved by the distribution system. A change in the flow area of the fuel mixture is achieved by setting the valve lift h depending on the rotational angle of the camshaft θc. Fig. 1 outlines a typical distribution system in which a cam (built on a camshaft) actuates a rocker arm through a roller, thereby moving the valve. A spring located between the valve and the motor housing keeps contacts valve-rocker, rocker-follower rod and roller cam follower. The rotation of the camshaft is provided by a power transmission system.

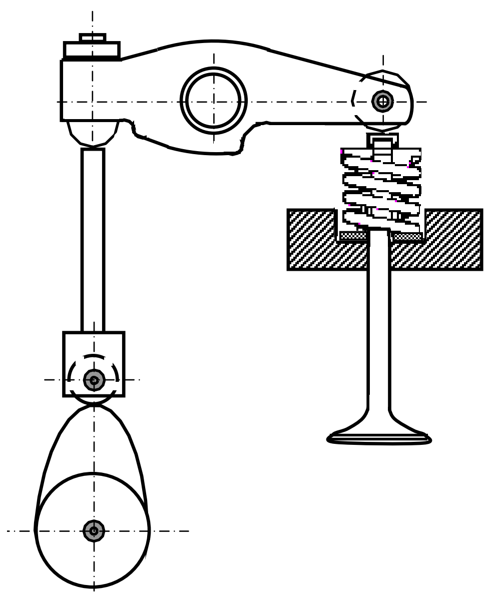

Fig.1. Conventional valve train

We propose in this study to address the dynamic behavior of a distribution system camshaft through a lumped parameters dynamic model. The advantage of this model (Fig. 2) compared to the existing models in the literature is to replace the follower plate by a roller follower to minimize friction. On the other hand, this model takes into account the nonlinear Hertzian stiffness between cam and follower, whereas constant contact stiffness is considered between valve and rocker and between rocker and follower rod. The cam follower model with 8 degrees of freedom is derived from the work of Kim [12].

This mechanism consists of a cam, a follower roller and a load represented by the displaced mass M_1 which models the valve. The return spring K_{rs} allows permanent maintaining in contact between the different elements. The rocker is considered as a rigid body. The shaft bearings, cam rollers, and the follower arm are modeled by linear springs, damping is introduced in parallel with the springs. The elastic contact between the cam and the follower (roller 1) is modeled by a nonlinear spring acting along the line of action (normal through the point of contact and defined by the pressure angle α. The contact between the rocker and the valve is provided by the roller 2. The follower is modeled by two masses connected together by a spring and damping.

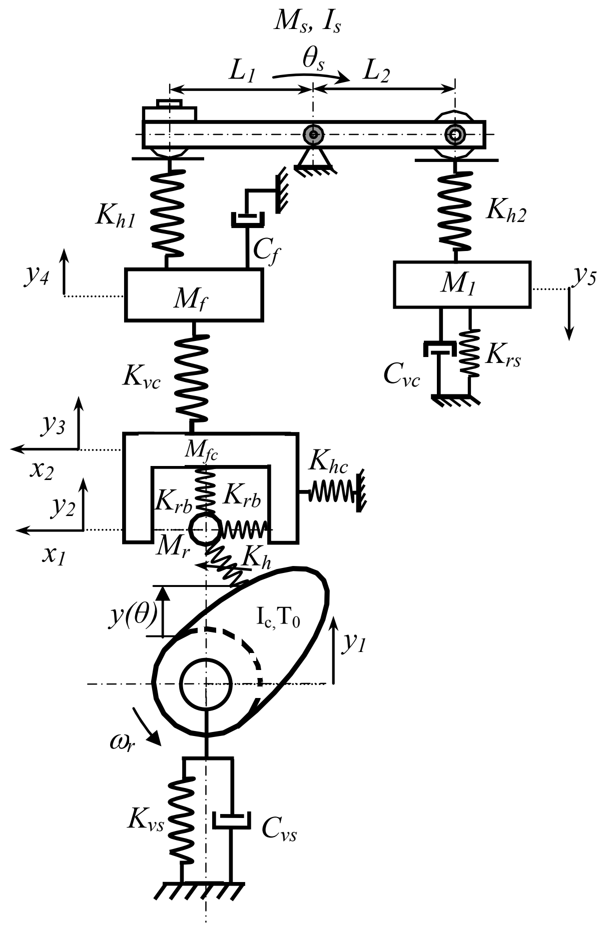

Fig. 2. 8 degrees of freedom model of the valve train

After computing the expressions of kinetic, strain and dissipative energies, the equations of motion can be recovered by applying Lagrange formulation. The different equations of motion can be written by :

$$
\begin{aligned}
& I_s \ddot{\theta}_s - L_1 C_{h1} \dot{y}_4 + \left(L_1^2 C_{h1} + L_2^2 C_{h2}\right)\dot{\theta}_s + L_2 C_{h2} \dot{y}_5 - L_1 K_{h1} y_4 + \left(L_1^2 K_{hl} + L_2^2 K_{h2}\right)\theta_s + L_2 K_{h2} y_5 = 0 \\
& M_c \ddot{y}_1 + C_{vs} \dot{y}_1 + K_{vs} y_1 = -F_c \cos\alpha \\
& M_r \ddot{y}_2 - K_{rb}(y_3 - y_2) = F_c \cos\alpha \\
& M_{fc} \ddot{y}_3 + K_{rb}(y_3 - y_2) - K_{vc}(y_4 - y_3) = 0 \\
& M_f \ddot{y}_4 + C_{h1}(L_1 \dot{\theta}_s + \dot{y}_4) + C_f \dot{y}_4 + K_{h1}(L_1\theta_s + y_4) + K_{vc}(y_4 - y_3) = 0 \\
& M_l \ddot{y}_5 + L_2 C_{h2} \dot{\theta}_s + \left(C_{h2} + C_{vc}\right)\dot{y}_5 + L_2 K_{h2}\theta_s + \left(K_{h2} + K_{rs}\right) y_5 = F_P \\
& M_c \ddot{x}_1 + C_{hs} \dot{x}_1 + K_{hs} x_1 = F_c \sin\alpha \\
& M_r \ddot{x}_2 + K_{rb}(x_2 - x_3) = -F_c \sin\alpha \\
& M_{fc} \ddot{x}_3 + K_{hc} x_3 - K_{rb}(x_2 - x_3) = 0
\end{aligned} \tag{1}
$$

It is possible to write this system of equations by :

$$[M]\{\ddot{q}\} + [C]\{\dot{q}\} + [K]\{q\} = \{F\} \tag{2}$$

Where $\{q\}$ is the vector of the degrees of freedom given by:

$$\{q\} = \{\theta_S \quad y_1 \quad y_2 \quad y_3 \quad y_4 \quad y_5 \quad x_1 \quad x_2\}^T \tag{3}$$

is the mass matrix expressed by :

$$
[M] = \begin{bmatrix}
I_S & & & & & & & \\
& M_c & & & 0 & & & \\
& & M_r & & & & & \\
& & & M_{fc} & & & & \\
& & & & M_f & & & \\
& & & & & M_l & & \\
& 0 & & & & & M_r & \\
& & & & & & & M_c
\end{bmatrix} \tag{4}
$$

The damping matrix $[C]$ is given by:

$$
[C] = \begin{bmatrix}
L_1^2 C_{h1} + L_2^2 C_{h2} & 0 & 0 & 0 & L_1 C_{h1} & L_2 C_{h2} & 0 & 0 \\
0 & C_{vs} & 0 & 0 & 0 & 0 & 0 & 0 \\
0 & 0 & 0 & 0 & 0 & 0 & 0 & 0 \\
0 & 0 & 0 & 0 & 0 & 0 & 0 & 0 \\
C_{h1} L_1 & 0 & 0 & 0 & C_{h1} + C_f & 0 & 0 & 0 \\
C_{h2} L_2 & 0 & 0 & 0 & 0 & C_{h1} + C_{vs} & 0 & 0 \\
0 & 0 & 0 & 0 & 0 & 0 & 0 & 0 \\
0 & 0 & 0 & 0 & 0 & 0 & 0 & 0
\end{bmatrix} \tag{5}
$$

The stiffness matrix $[K]$ is expressed by:

$$
[K] = \begin{bmatrix}
L_1^2 K_{hl} + L_2^2 K_{h2} & 0 & 0 & 0 & -L_1 K_{h1} & L_2 K_{h2} & 0 & 0 \\
0 & K_{vs} & 0 & 0 & 0 & 0 & 0 & 0 \\
0 & 0 & K_{rb} & -K_{rb} & 0 & 0 & 0 & 0 \\
0 & 0 & -K_{rb} & K_{rb} + K_{vc} & -K_{vc} & 0 & 0 & 0 \\
-K_{h1} L_1 & 0 & 0 & -K_{vc} & K_{vc} + K_{h1} & 0 & 0 & 0 \\
K_{h2} L_2 & 0 & 0 & 0 & 0 & K_{h2} + K_{rs} & 0 & 0 \\
0 & 0 & 0 & 0 & 0 & 0 & K_{rb} & -K_{rb} \\
0 & 0 & 0 & 0 & 0 & 0 & -K_{rb} & K_{hc} + K_{rb}
\end{bmatrix} \tag{6}
$$

The external applied forces vector is:

$$
\{F\} = \begin{Bmatrix}
0 \\ -F_c \cos\alpha \\ F_c \cos\alpha \\ 0 \\ 0 \\ F_P \\ -F_c \sin\alpha \\ 0
\end{Bmatrix} \tag{7}
$$

F_c is the contact force between cam and follower, F_p is the preload applied on K_{rs} to maintain contact.

3 Modeling of camshaft eccentricity and cam profile error

One of the major defects that can occur during machining process of camshafts is the eccentricity. It can be defined as the difference between the geometrical rotational axis and the actual one.

To model eccentricity defect, an error $e_c(t)$ having amplitude that varies in sinusoidal shape at the rotational frequency ω_r of the camshaft is considered. Its expression is given by:

$$e_c(t) = \overline{e_c} \sin\left(\omega_r t + \zeta\right) \tag{8}$$

where $\overline{e_c}$ is the maximal amplitude of eccentricity. Fig. 3 shows the influence of eccentricity on geometrical parameters of the systems.

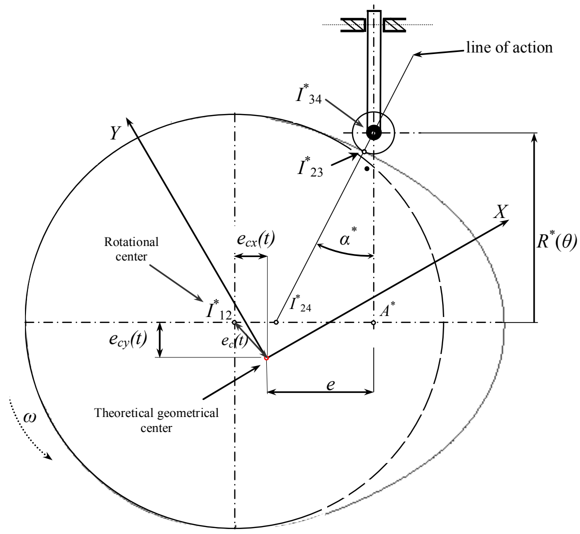

Fig. 3. Effect of eccentricity on position vector coordinates

It is well observed a shift of the pressure angle and an offset variation ($\Delta\alpha$ and Δe). The instantaneous contact point varies from I_{23} to I^*_{23} with corresponding angle θ. The new position vector $R^*_T(\theta)$ of point I^*_{23} in term of the cam rotation angle can be expressed as:

$$R^*_T(\theta)=\begin{Bmatrix} R^*_{T_x}(\theta) \\ R^*_{T_y}(\theta) \end{Bmatrix}=I^*_{12}I_{23}^{*}$$
$$I^*_{12}I_{23}^{*}=\begin{Bmatrix} R^*(\theta)\cos\theta-e^*\sin\theta-r_r\cos(\theta-\alpha^*) \\ R^*(\theta)\sin\theta+e^*\cos\theta-r_r\sin(\theta-\alpha^*) \end{Bmatrix} \tag{9}$$

Where

$$e^*=e\pm\Delta e_x$$

$$R^*(\theta)=\sqrt{(r_b+r_r)^2-e^{*2}}+h(\theta)$$

The pressure angle which depends of the new position vector will be expressed as follow:

$$\alpha^*=\tan^{-1}\left(\frac{I^*_{12}I_{24}^{*}-e^*}{R^*(\theta)}\right) \tag{10}$$

The profile error can be induced by several causes such as machining process, wear,…. It can be modelled by a sinusoidal error affecting the ideal profile of the cam as suggested by McAdams[13]:

$$e_p=(t_p/3)\sin(n\omega_r t) \tag{11}$$

where t_p is the profile tolerance, n is a small integer.

4 Numerical simulations

The studied valve train has the properties given in tables 1 and 2

	Follower motion			
	Dwell	Rise	Return	Dwell
angle	0 ~ 90°	90° ~ 180°	180° ~ 270°	270° ~ 360°
Profile		Cycloïdal	Cycloïdal	

Table 1. Motion cycle of the follower

Polar moment of inertia of rocker (kg.m^2)	0.00032
Mass (Kg)	M_c=0.9; M_r=0.023; M_l=1.36 ; M_{fc}=0.068 ; M_f=0.3
Linear damping coefficients (N.sec/m)	C_{vc}= 0.05 ; C_{h1}= C_{h2} = 0.125, C_f=0.075
Linear stiffness (N/m)	K_{hs} = K_{rb}= K_{vs}=K_{hc}= 2.6 10^8 ; K_{h1}=K_{h2}=1.1 10^8 ; K_{rs}=9.4 10^4 ; K_{vc}=1.75 10^8
Initial deformation of spring K_{rs} (mm)	δ_{rs}=10
The total rise (mm)	y_{max}=6
Diameter of cam base circle (mm)	R_b= 18
Diameter of follower roller (mm)	R_l=8
L1 (mm)	20
L2 (mm)	50

Table 2. Parameters of the valve train

4.1 Modal analysis

The resolution of the eigenvalue problem yields to the eigenfrequencies given in table 3.

Frequency (Hz)	$f_1 = 39$	$f_2 = 2521$	$f_3 = 2701$	$f_4 = 2701$
Type	RR+VTF	RR+VTF	CT	CT
Frequency (Hz)	$f_5 = 5340$	$f_6 = 7956$	$f_7 = 17009$	$f_8 = 20168$
Type	RR+VTF	RR+VTF	RLT	RR+VTF

Table 3. Eigenfrequencies of the system

When observing the eigenfrequencies, the following classification can be stated:

- Five eigenfrequencies (f1, f2, f5, f6 and f8) where the mechanism exhibit combined rocker rotation and vertical translation of the follower in the corresponding eigenvectors. Except for f8, the dominant modal deflection is the rocker rotation.
- A double eigenfrequency where a pure modal deflection of the cam is observed in the horizontal and the vertical directions.
- One eigenfrequency in which only the roller presents a modal deflection in the horizontal direction

4.2 Dynamic response simulation for the healthy case

The rotational speed of the camshaft is 800 rpm. Fig. 4 shows the evolution of the angular position of the rocker (θs) over time compared to the theoretical angle if the transmission considered rigid. It is found that the dynamic angular position of the rocker follows perfectly the theory which gives the system proper function.

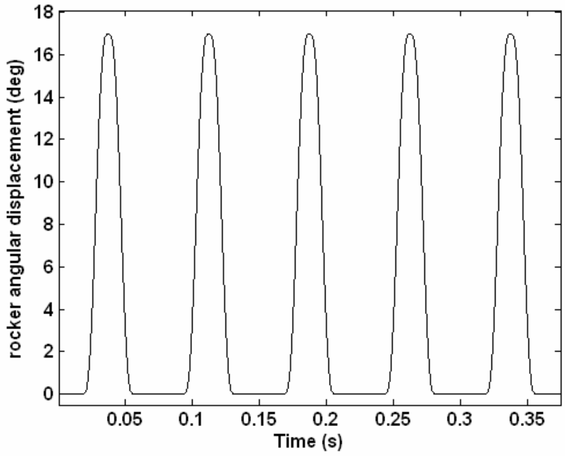

Fig. 4. Evolution of the angular position of the rocker

Fig. 5 shows the angular acceleration of the rocker over some cycles and Fig. 6 shows its spectrum.

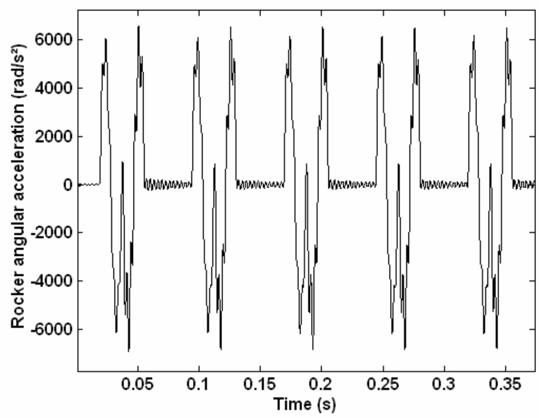

Fig. 5. Acceleration of the rocker

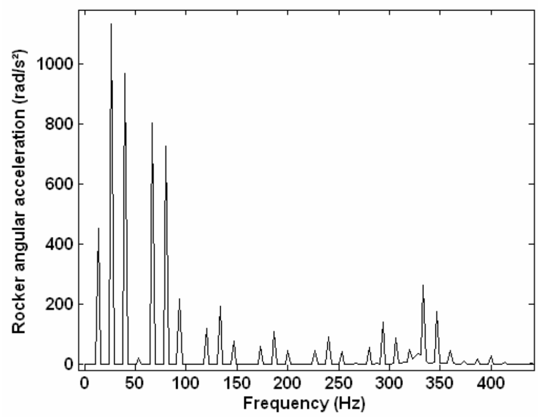

Fig. 6. Spectrum of evolution of the acceleration of the rocker

It is well observed a rapid fluctuation of the acceleration of the rocker which reached values around 6000m/s². A change in the acceleration sign is also observed. This is a normal behaviour seen the chosen profile of the cam. The spectrum of the acceleration shows the dominance of the rotational frequency of the camshaft (f_r = 13.33 Hz) and its harmonics with increasing amplitudes around eigenfrequency f_2 in which the modal deflection consists in a combined rocker rotation and vertical translation of the follower. The displacement of the valve is given in Fig. 7.

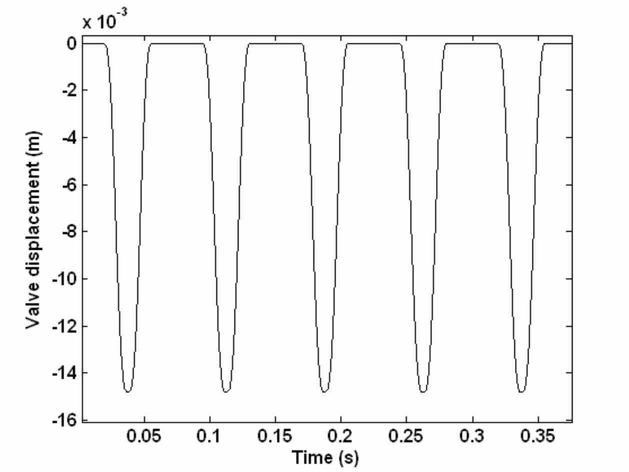

Fig. 7. Valve displacement evolution

The valve reached its maximum value (-14.8 mm) after 0.017 seconds. This time is convenient for the chosen rotational speed and allows the valve to perform its mission during the cycle of intake or exhaust. The acceleration of the valve and its spectrum are represented in Fig.s 8 and 9.

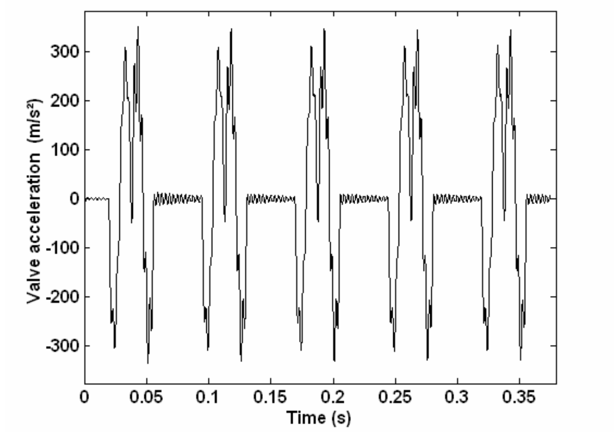

Fig. 8. Valve acceleration evolution

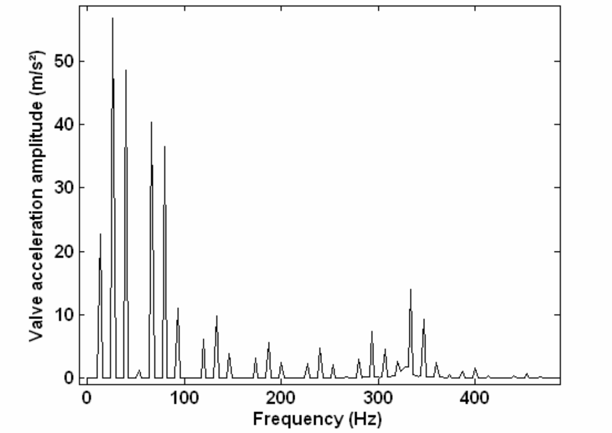

Fig. 9. Spectrum of the valve evolution

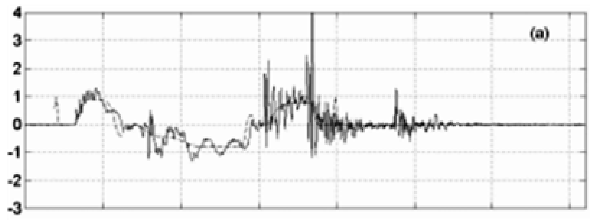

Fig. 10. Experimental acceleration measure of a valve [10]

Acceptable values of the valve accelerations are observed not exceeding 300 m/s². The spectrum shows components at 1xf_r and harmonics. When comparing Fig. 5 and 8 one can observe the same shape of spectrum (but with different amplitudes). This confirms the vibration transmission from rocker to valve. The acceleration exhibit similar behaviour to that obtained experimentally by Carlini [10] (Fig. 10).

Let's now look at the contact force between the rocker and valve F_{c1}. This force can be expressed as follows:

$$Fc_1 = Kh_2\left(y_5 - L_2\theta_s\right) \quad (12)$$

Fig. 11 shows the evolution of F_{c1} and Fig. 12 the corresponding spectrum.

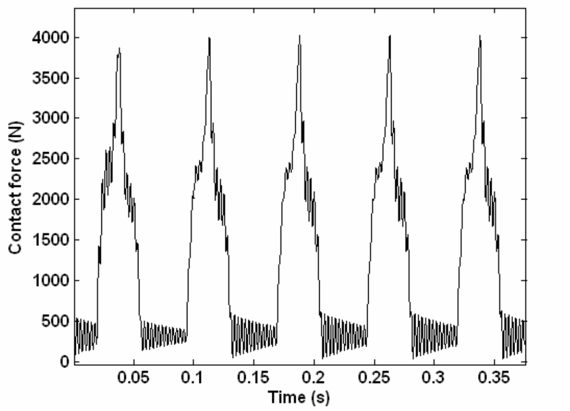

Fig. 11 Time evolution of the rocker-valve contact force

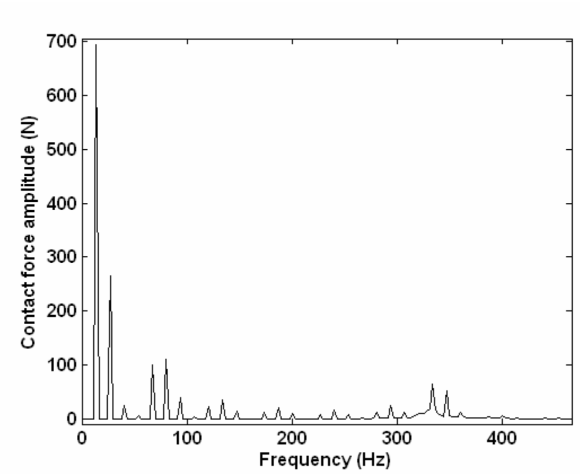

Fig. 12. Spectrum of the rocker-valve contact force

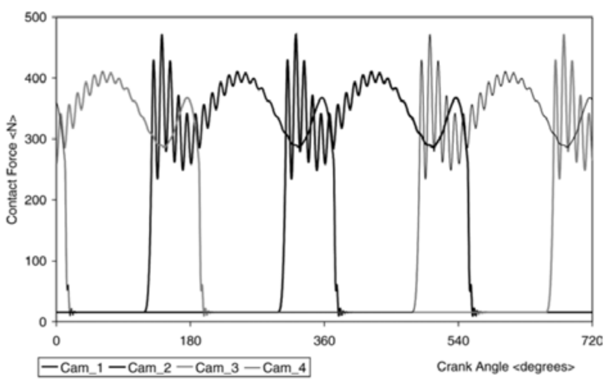

Fig. 13. Experimental values a cam-rocker contact force [9]

The mean value of the force is about 300N when the cam is in the dwell phase and reaches important values around 4000N when the valve is at its lower position (-14.8 mm). These positive values indicate that there is always contact. A fluctuation is observed which follows the fluctuations registered on follower and valve accelerations. The spectrum of the contact force indicates the dominance of the fundamental component of rotations frequency. Results can be validated by the work made by Teodorescu [9] who found rapid fluctuations of this contact force (Fig.13).

4.3 Dynamic response simulation for the eccentricity defect

An eccentricity defect $\overline{e_c}=5.10^{-6}$mm was introduced in the model. The influence of this defect on the displacement of the valve is given by Fig. 14 the amplitude of fluctuations on the dwell phase increase slightly.

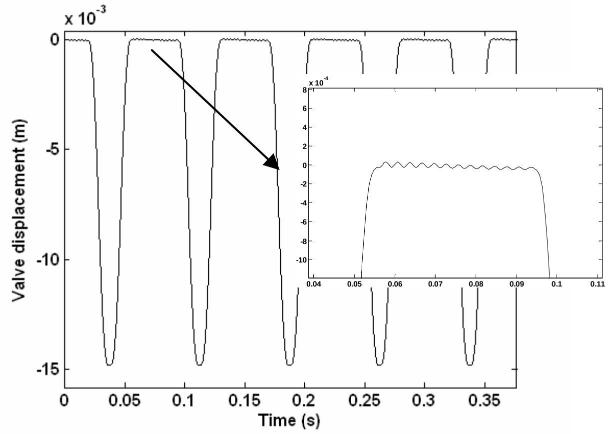

Fig. 14. Time evolution of valve displacement in presence of the eccentricity error

The acceleration curve of the valve confirms this fluctuation with moderate increase in accelerations on this part as presented in Fig. 15 the corresponding spectrum (Fig.16) confirms this increase especially in higher order harmonics.

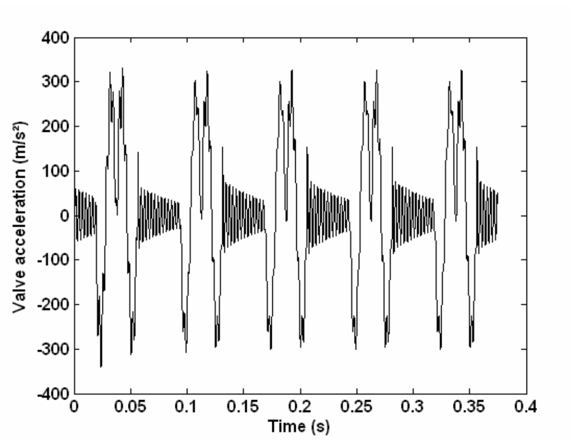

Fig. 15 Acceleration of the valve for the eccentricity defected case

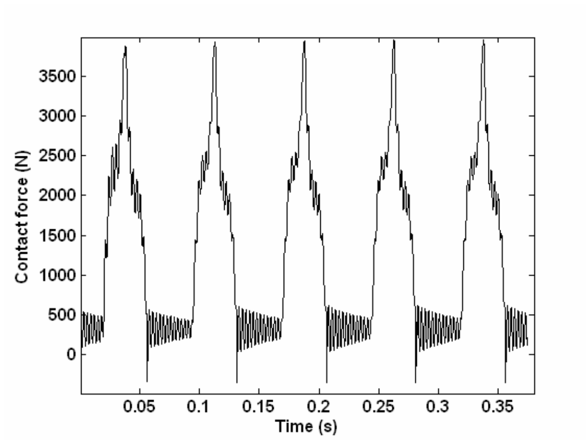

Fig. 17 Time evolution of the follower-rocker contact force in presence of the defect

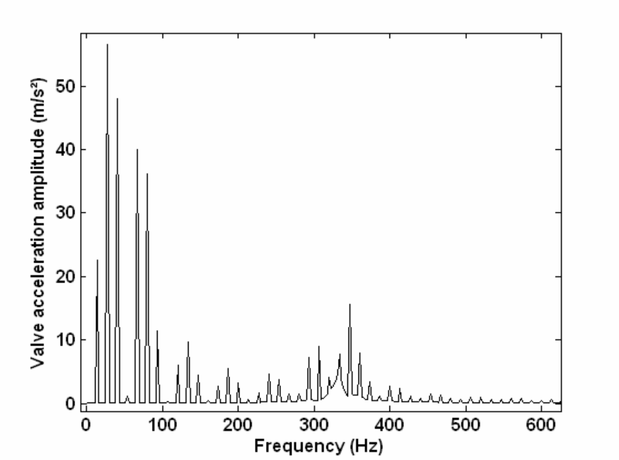

Fig. 16. Spectrum of the acceleration of the valve for the defected case

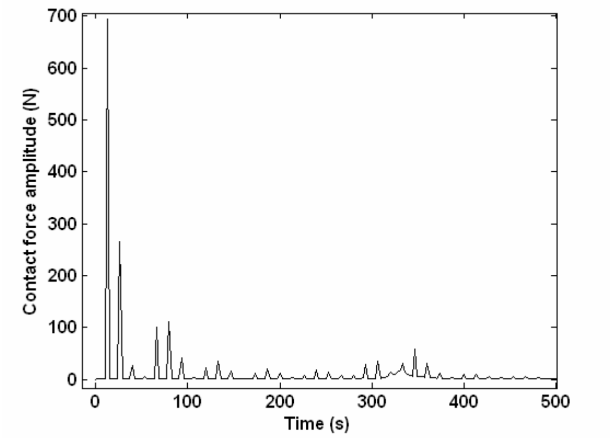

Fig. 18. Spectrum of contact force signal for the eccentricity error

As a consequence, the rocker-valve contact force is expected to increase in dwell phase. Fig. 17 shows the evolution of Fc_1 with higher amplitudes of forces especially during the dwell phase and a risk of contact loss between valve and rocker at the end of the valve return phase. The spectrum of the contact force evolution (Fig. 18) shows also a small increase of components at higher order harmonics of f_r.

4.4. Dynamic response simulation for the profile error defect

A profile error of with t_p=8.10^{-6} and n=30 is considered at the cam profile. The dynamic response is computed. Fig. 19 shows the evolution of the cam displacement. The zoom presented in this figure show clearly a high fluctuation of this displacement in the dwell zone which implies an unstable stay of the valve in its seat which may alters the sealing of the combustion chamber.

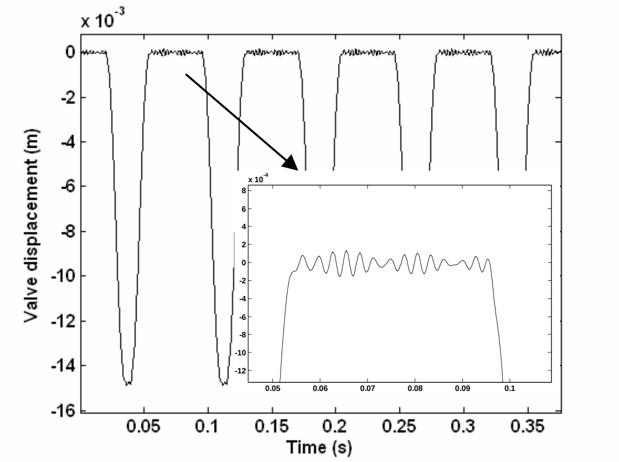

Fig. 19. Time evolution of valve displacement in presence of the profile error

Fig. 20 shows the acceleration of the valve. It is well noticed that the high vibration levels with rapid fluctuations reaching 1000 m/s². This was mainly caused by the irregularities of the cam surface which is transferred to the valve by the follower and the rocker. The spectrum of the valve acceleration (fig21) confirms this change by increased values of rotational frequency harmonics.

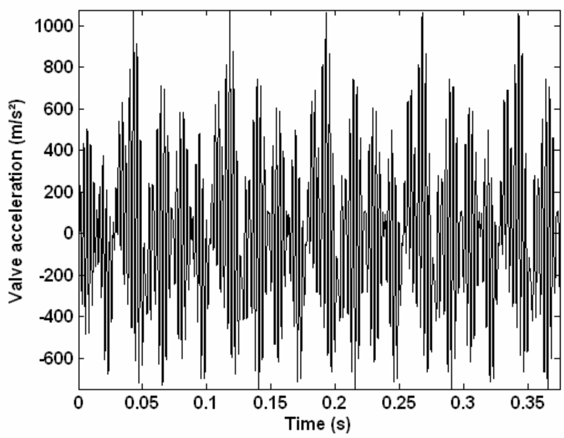

Fig. 20. Acceleration of the valve in presence of the profile error

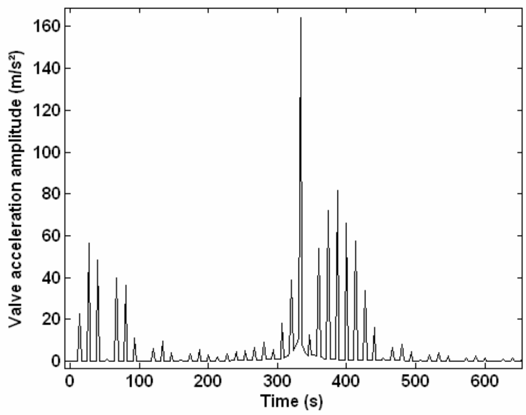

Fig. 21. Acceleration of the valve in presence of the profile error

As a consequence, the contact forces between the valve and the rocker increases to reach 8000 N with many fluctuations (fig 22) associated with increase of higher harmonics amplitudes (Fig. 23). This phenomenon can be harmful for the transmission.

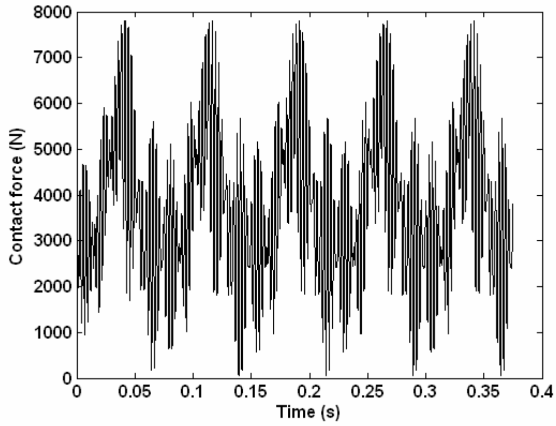

Fig. 22. Contact force evolution in the case of profile error

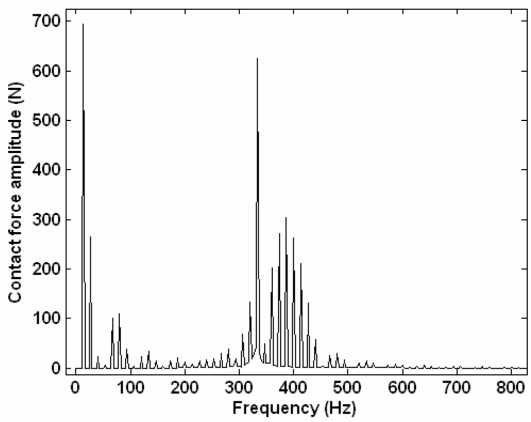

Fig. 23. Spectrum of the contact force evolution in the case of profile error

5. Conclusions

In this paper a cam-follower-rocker-valve mechanism was presented. It was modelled by 8 degrees of freedom model. The effect of eccentricity of the camshaft and the profile errors of the cam surface was also modelled and introduced to the model. Numerical simulations of the dynamic behaviour of the system lead to the following major remarks:

- The dynamic behaviour of the system is mainly induced by the cam profile with its specific displacements and acceleration.

- The rocker and valve dynamic behaviour is correlated to the cam follower dynamic response

- Moderate contact forces and accelerations of the valve are observed for the healthy case

- For camshaft eccentricity defect, a slight increase in the vibration level is observed particularly in the dwell phase.

- For the profile error defect, it was observed a substantial change in the vibration levels associated with increases in the contact force between the valve and the rocker.

References

[1] Heisler, H., *Advanced Engine Technology*, Butterworth- Heinmann, Second Edition, 2002.
[2] Husselman M, *Modelling and verification of valve train dynamics in engines*, MSc, Stellenbosch University, 2005
[3] Norton, R. L., Mosier R. G., *Cam Design and Manufacturing Handbook*, Industrial Press, Inc., New York, 2002.
[4] David, J.W., Cheng, C.Y., Choi, T.D., Kelley, C.T., Gablonsky J., Optimal Design of High Speed Mechanical Systems, North Carolina State University, Tech. Rep. CRSC-TR97-18, 1997
[5] Choi, T. D., Eslinger, C. T. Kelley, O. J.,. David, J. W, Etheridge M., Optimization of Automotive Valve Train Components with Implicit Filtering, *Optimization and Engineering*, 2000, 3, 9–27.
[6] Cardona, A., Lens, E. and Nigro, N., Optimal Design of Cams, *Multibody System Dynamics*, 2002, 7, 285–305.
[7] Kim, W.J., Jeon, H.-S. and Park, Y.S., Contact Force Prediction and Experimental Verification on an OHC Finger-follower type Cam valve System, *Experimental Mechanics* , 1991, 31(2), 150-156.
[8] Jeon, H.S, Park, K.J. and Park, Y.-S, An Optimal Cam Profile Design Considering Dynamic Characteristics of a Cam valve System, *Experimental Mechanics*, 1989, 29(4), 357-363.
[9] Teodorescu, M., Kushwaha, M., Rahnejat, H., and Taraza, D., Elastodynamic transient analysis of a four-cylinder valve train system with camshaft flexibility, Proc. IMechE Part K: J. Multi-body Dynamics, 219, 13-25.
[10] Carlini, A., Rivola, A. Dalpiaz, G. Maggiore, A., Valve motion measurements on motorbike cylinder heads using high speed laser vibrometer, Proceedings of the 5th International Conference on Vibration Measurements by Laser Techniques: Advances and Applications, Ancona (Italy), 2002, 564–574.
[11] De Wilde, E. F., Investigation of Engine Exhaust Valve Wear, *Wear*, 1967, 10(3), 231-244.
[12] Kim, H.R., Newcombe, W.R., The effect of cam profile errors and system flexibility on cam mechanism output, *Mechanism and Machine Theory*, 1982, 17, 57–72.
[13] McAdams, D. A., Tumer, I. Y., Towards Failure Modelling in Complex Dynamic Systems: Impact of Design and Manufacturing Variations, Proceedings of DETC'02, 2002 ASME Design Engineering Technical Conferences, September 29-October 2, 2002, Montreal, Quebec, Canada.